RSC Advances

Journal Name

RSC Advances

Dynamic Article Links ▶

ARTICLE TYPE

Organic Thin Film Transistors with Novel Photosensitive Polyurethane as Dielectric Layer

Yao Li[1], He Wang[2], Xuehui Zhang[1], Qiong Zhang[1], Xuesong Wang[1], Danfeng Cao[1], Zuosen Shi[1], Donghang Yan*[2] and Zhanchen Cui*[1]

In this paper, we report the design, synthesis, and dielectric properties of novel photosensitive polyurethane dielectric film used in organic thin-film transistors (OTFTs). The novel photosensitive polyurethane dielectric film is readily fabricated by spin coating followed by curing at UV light. The film
10 exhibits excellent insulating properties, smooth surface, and excellent photosensitive property. The bottom-gate top-contact para-sexiphenyl (*p*-6P)/ vanadyl-phthalocyanine (VOPc) OTFTs with photosensitive polyurethane films as the dielectric layer exhibit excellent performance with mobility of 0.13 cm^2/Vs, on/off ratio of 10^4 and ultralow leakage.

1. Introduction

15 Unlike conventional inorganic technology, organic thin-film transistor (OTFT)-based electronics performing simple operations provide unique qualities, including low cost, large-area coverage, and low processing temperatures[1-6]. In particular, para-sexiphenyl (*p*-6P)/ vanadyl-phthalocyanine (VOPc) OTFTs have attracted
20 considerable attention and have already demonstrated their potential toward organic electronic applications[7-10]. However, the critical issue that limits the performance of *p*-6P/ VOPc OTFTs is its large leakage current. The dielectric layer, as an important part of OTFTs, can effectively influence the leakage current and
25 performance of these devices. One approach to reducing leakage current is the use of novel organic/inorganic dielectric materials as dielectric layer[11-14]. Furthermore, OTFTs have been fabricated by using high-density self-assembled monolayers (SAMs) dielectric films as dielectric layer[15-18]. These methods exhibit
30 excellent insulating properties and have been successfully used in OTFTs. However, current pathways for the integration of these layers into large-area coating processes are inapplicable.
For large-area electronic applications, various solution-processable materials are chosen as dielectric layer because these
35 materials can be formed simply via spin-coating, casting, or printing at room temperature[19-22]. However, compared with traditional materials， insulation of solution-processable materials is not enough. Therefore, increasing the insulation of solution-processable materials is a major challenge in fabricating
40 large-area electronic applications of OTFTs. As reported, leakage current can be minimized due to the reduced free volume in the dielectric layer, which guaranteed a more active cross-linking reaction[23-25]. For cross-linking materials, one major choice is to employ an organic cross-linker in the solution-processable
45 materials solution. Another effective solution is the use of a novel polymer structure with cross-linked group, such as epoxy group[26].

The resulting OTFTs with these dielectric layer function at a low leakage current. However, the critical issue that limits application of these methods is a high temperature processes and a shorter
50 storage time. Therefore, it is necessary to develop cross-linking and low-temperature processable solution-processable materials as dielectric layers.
Photosensitive solution-processable materials are considered viable alternative materials that can simplify procedures and
55 reduce the manufacturing costs of large-area electronic applications[27, 28]. In particular, solution-processable polyurethane has attracted considerable attention, due to high tensile strength, excellent abrasion resistance and good mechanical properties[29]. In this work, to afford a photosensitive cross-linking solution-
60 processable material, we design and synthesis a novel monomer that contained hydroxy and olefin groups. This monomer can copolymerize with 4, 4'-methylenebis(cyclohexyl isocyanate), and 2, 2-bis butyl cinnamoylate (hydroxymethyl) to obtain a solution-processable photosensitive polyurethane. These
65 monomers can provide a more flexible structure to improve film-forming property of polyurethane. In this polyurethane, the olefin groups provide a more active cross-linking reaction by UV curable, and leakage current can be minimized due to the reduced free volume in the dielectric layer. The leakage current of *p*-6P/
70 VOPc OTFTs with the novel photosensitive polyurethane film as dielectric layer has a significantly decrease. In the same time, the good anchoring strength and flexibility of polyurethane provides high performance of OTFTs.

2. Experimental Section

2.1 Materials

75 Bis(2-hydroxyethyl)terephthalate, 4, 4'-methylenebis(cyclohexyl isocyanate), dibutyltin dilaurate and cinnamoyl chloride were obtained from Aldrich Chemical Co. 2-Ethyl-2-(hydroxymethyl)-

1, 3-propanediol was purchased from Alfa Chemical Co.
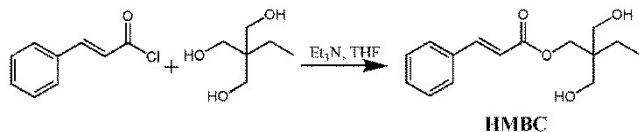
Scheme 1 The fabrication process of 2, 2-bis (hydroxymethyl) butyl cinnamoylate (HMBC).

## 2.2 Synthesis of 2, 2-bis (hydroxymethyl) butyl cinnamoylate (HMBC)

A solution of cinnamoyl chloride (1.66 g, 1 mmol) in tetrahydrofuran (THF) (30 mL) was added dropwise at 0 ℃ to the solution of 2-ethyl-2-(hydroxymethyl)-1, 3-propanediol (6.70 g, 5 mmol) and triethylamine (1.212 g, 12 mmol) in THF (100 mL). The temperature was kept in the ambient and the mixture was stirred for 12 h. After reaction completed, the reaction mixture was filtered to remove the solid, and the filtrate solution was concentrated. The resulting solid was purified by column chromatography over silica using Petroleum ether/ethyl acetate (3/2 v/v) to obtain HMBC (2.7 g, 90%). The preparation and structure of HMBC are illustrated in scheme 1.

The HMBC characterization: ^{1}H NMR (DMSO, 500 MHz): δ 7.77 − 7.69 (m, 2H), 7.65 (d, J = 16.1 Hz, 1H), 7.51 − 7.38 (m, 3H), 6.63 (d, J = 16.0 Hz, 1H), 4.45 (s, 2H), 4.02 (s, 2H), 3.35 (s, 4H), 1.34 (q, J = 7.5 Hz, 2H), 0.84 (t, J = 7.5 Hz, 3H). ^{13}C NMR (500 MHz, DMSO): δ 166.80 (s), 144.64 (s), 134.53 (s), 130.85 (s), 129.38 (s), 128.78 (s), 118.80 (s), 64.79 (s), 61.44 (s), 43.18 (s), 40.06 (d, J = 21.0 Hz), 39.83 (s), 39.81 (s), 22.18 (s), 7.90 (s). FT-IR (KBr, cm^{-1}): 3644-3093 (s, -OH), 3064 (vw, H-C=), 2964 (w, -CH$_3$), 2929, 2881 (w, -CH$_2$-), 1698 (s, -C=O), 1635 (s, -C=C), 1452, 1378 (m, benzene).

2.4 Synthesis of photosensitive polyurethane

HMBC (0.77 g, 3 mmol), 4, 4'-methylenebis(cyclohexyl isocyanate) (2.62 g, 10 mmol), bis(2-hydroxyethyl)terephthalate (2.27 g, 9 mmol) and 200 mL THF were mixed. Under N$_2$ atmosphere, dibutyltin dilaurate (0.1 g) was then added as initiator. The mixture was refluxed for 12 h 70 ℃. After cooling to room temperature, the above solution was added to hexane and white solid formed. This step was repeated three times and then was dried in a vacuum to obtain photosensitive polyurethane (4.69 g, 83%). The preparation, structure and UV curable process of photosensitive polyurethane are illustrated in scheme 2.

The photosensitive polyurethane characterization: ^{1}H NMR (DMSO, 500 MHz): δ 8.07 (d, J = 20.3 Hz, 36H), 7.66 (d, J = 16.2 Hz, 3H), 6.64 (d, J = 15.9 Hz, 3H), 3.61 (t, J = 6.2 Hz, 20H). ^{13}C NMR (500 MHz, DMSO): δ 165.33 (s), 40.09 (d, J = 20.9 Hz), 39.84 (s), 25.59 (s), 7.85 (s). FT-IR (KBr, cm^{-1}): 3698-3093 (s, -OH), 3060 (vw, H-C=), 2925 (w, -CH$_3$), 2854 (w, -CH$_2$-), 1724 (s, -C=O), 1641 (s, -C=C), 1452, 1378 (m, benzene).
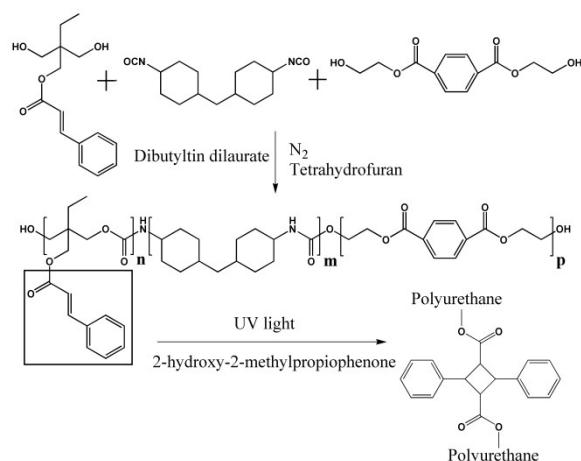
Scheme 2 The fabrication and UV curable process of photosensitive polyurethane.

2.5 Device Fabrication

To determine the capacitance and gate leakage of the film, 15% photosensitive polyurethane solution with 0.5% 2-hydroxy-2-methylpropiophenone was spin coated on top of ITO wafer. The films were annealed at 80 ℃ for 10 min to remove all the solvent and then were irradiated by UV light for 10 min. Finally, the MIM devices were prepared after evaporating the top Au electrode in a radius of 1 cm round area. The final thickness of the photosensitive polyurethane films was 690 nm.

As shown in Figure 1, a bottom-gate top-contact OTFT device geometry was used in all the electrical characterizations. The photosensitive polyurethane was deposited on the ITO wafer by spin-coating as dielectric layer. The thickness of the films was 690 nm. A 3 nm *p*-6P layer was deposited on the surface of polymer film, and then 30 nm VOPc film was deposited on *p*-6P layer. All organic thin films were deposited at 10^{-4}~10^{-5} Pa at a rate of about 1 nm min^{-1} and the substrate temperature was kept at 180 ℃. The wafers were rapidly transferred to another vacuum chamber to define the source and drain contacts by thermally evaporating Au with a mask shadow in vacuum at 10^{-4} Pa to complete the fabrication of organic field-effect transistors. The width and length of the transistor channels were 6000 μm and 200 μm, respectively.

Fig. 1 Schematic of a bottom-gate top-contact para-sexiphenyl (*p*-6P) / vanadyl-phthalocyanine (VOPc) OTFTs device geometry.

2.6 Measurements

Nuclear magnetic resonance (NMR) spectra were performed on a Bruker AVANCE NMR spectrometer at a resonance frequency of 500 MHz for ^{1}H NMR. The chemical shifts of ^{1}H NMR spectra

Journal Name

ARTICLE TYPE

were referenced to TMS at 0 ppm. IR spectra were taken on an AVANAR 360 FTIR infrared spectrophotometer. The molecular weights and molecular weight distributions were determined by gel permeation chromatography (GPC) on a Waters 410 GPC
5 with polystyrene as the standard and THF as the solvent at 40 °C at a flow of 1.0 mL/min. Differential scanning calorimetry (DSC) was determined with NETZSCH DSC 204 analyzer at a heating rate of 10 °C min^{-1} in a nitrogen atmosphere. The decomposition temperature thermogravimetric analysis (TGA) was obtained on a
10 PerkinElmer TGA 7 thermogravimetric analyzer. Atomic force microscopy (AFM) observations of the film surfaces were carried out with a commercial instrument (Digita Instrument, Nanoscope IIIa, Multimode) under ambient conditions at room temperature. All images were recorded under ambient conditions in the
15 tapping mode using a scan speed of 1 Hz. All the RMS surface-roughness values were reported in the area of $10 \times 10 \ \mu m^2$. Scanning electron microscopy (SEM) was performed on a JEOL FESEM 6700F electron microscope with primary electron energy of 2 kV. The capacitance of the photosensitive polyurethane was
20 measured with an Agilent E 4980A LCR meter. Current-voltage measurements were performed under ambient conditions at room temperature with the two Keithley 236 source-measurement units.
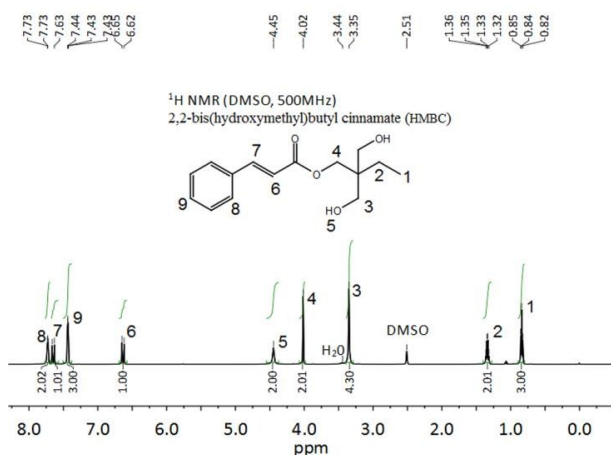

Fig. 2 The ^{1}H NMR spectrum and structure of 2, 2-bis (hydroxymethyl)
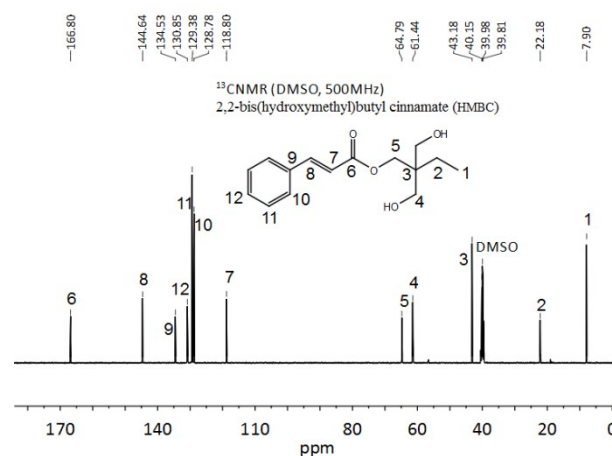25 butyl cinnamoylate (HMBC) (DMSO, 500 MHz,).

Fig. 3 The ^{13}C NMR spectrum and structure of 2, 2-bis (hydroxymethyl) butyl cinnamoylate (HMBC) (DMSO, 500 MHz,).
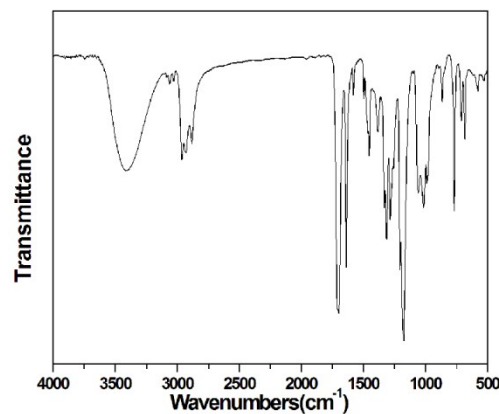

30 **Fig. 4** The FT-IR spectrum of 2, 2-bis (hydroxymethyl) butyl cinnamoylate (HMBC).

3. Results and Discussion

3.1 Structural characterization

We prepared HMBC with hydroxy and olefin groups. The novel
35 monomers were isolated as yellow solids and their structures were confirmed by ^{1}H NMR, ^{13}C NMR and FT-IR. The ^{1}H NMR spectrum and organic structure of HMBC was shown in Figure 2. The signals around 7.77–7.69 and 7.51–7.38 ppm were attributed to the hydrogen atoms in benzene, and the characteristic peaks
40 around 7.65, 6.63 ppm were assigned to the protons on the olefin groups. In the ^{13}C NMR spectrum of HMBC (Figure 3), two signals at 118.8 and 144.6 ppm were attributed to the carbon atoms of aliphatic double bond. FT-IR spectrum of HMBC was shown in Figure 4. The hydroxy group absorption was assigned
45 to 3644-3093 cm^{-1}. Furthermore, the characteristic absorption of amide carbonyl group was observed in 1698 cm^{-1}. These results

indicate that HMBC has been synthesized successfully. At the same time, the ^{1}H NMR spectrum organic structure of the photosensitive polyurethane was shown in Figure 5. The 7.66 and 6.64 ppm signals were ascribed to the characteristic peaks of the HMBC. The 8.07 and 3.61 ppm signals corresponded to the hydrogen atoms of the 4, 4'-methylenebis(cyclohexyl isocyanate) and bis(2-hydroxyethyl)terephthalate, respectively. As shown in Figure 6, the characteristic peaks of methyl carbon, cyclohexane carbon, and carboxyl carbon were observed at 7.85, 25.59, and 165.33 ppm in ^{13}C NMR spectrum of photosensitive polyurethane, respectively. In the FT-IR spectrum (Figure 7), the absorption of 3698-3093 cm^{-1} was attributed to the hydroxyl group of the photosensitive polyurethane; the peak at 2854 cm^{-1} was due to the antisymmetric stretching absorption of methylene. The characteristic peak of carbon-carbon double bond in 1641 cm^{-1} was disappeared after the UV light, indicating the cross-linking reaction has already happened by the double bond in the structure of polyurethane. These results indicate that we have successfully introduced the photosensitive groups into the polyurethane.
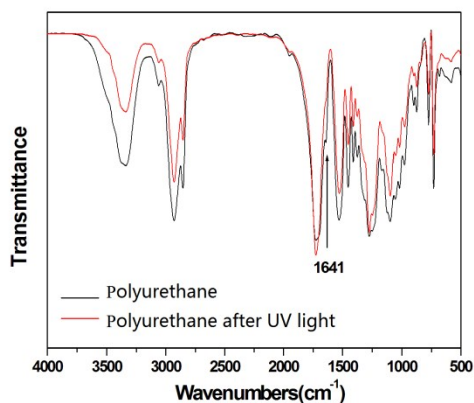

Fig. 7 The FT-IR spectrum of the photosensitive polyurethane.

3.2 Thermal analysis

The cross-linking behavior of the photosensitive polyurethane was investigated by differential scanning calorimetry, the result of which was shown in Figure 8. The glass transition temperature (T_g) of photosensitive polyurethane was 123 ℃. When the photosensitive polyurethane was cross-linked by UV light, the characteristic curve of the glass transition temperature disappeared, thus suggesting that photosensitive polyurethane was completely cured. The cured film of photosensitive polyurethane was transparent and insoluble in any organic solvents. The thermostability of the cured photosensitive polyurethane was evaluated by thermogravimetric analysis (TGA) (Figure 9). The cured photosensitive polyurethane has high thermostability, with thermal decomposition occurring at around 335 ℃.
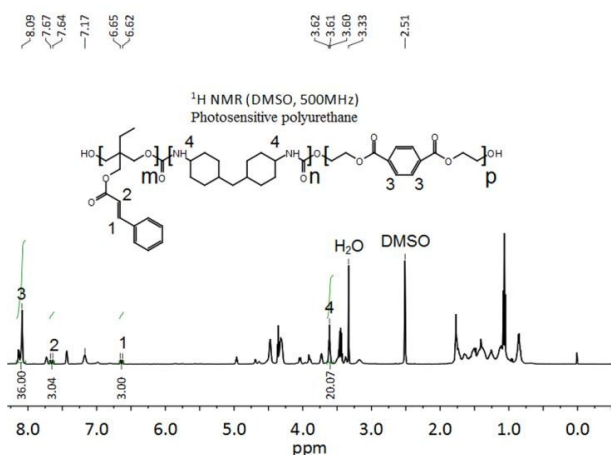

Fig. 5 The ^{1}H NMR spectrum and structure of the photosensitive polyurethane (DMSO, 500 MHz,).
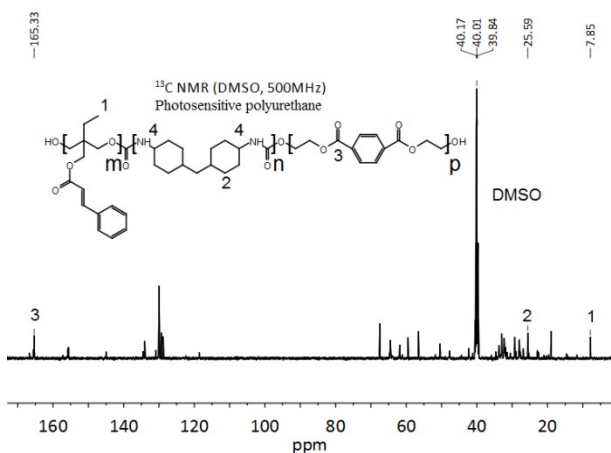

Fig. 6 The ^{13}C NMR spectrum and structure of the photosensitive polyurethane (DMSO, 500 MHz,).
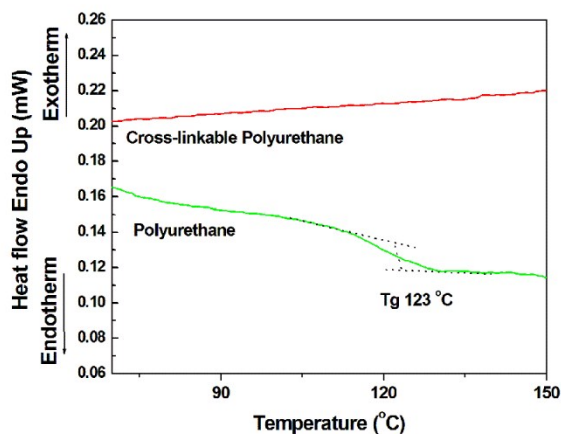

Fig. 8 DSC result of the photosensitive polyurethane with a heating rate of 10 ℃ min^{-1} in N$_2$.

Journal Name

RSC Advances

ARTICLE TYPE
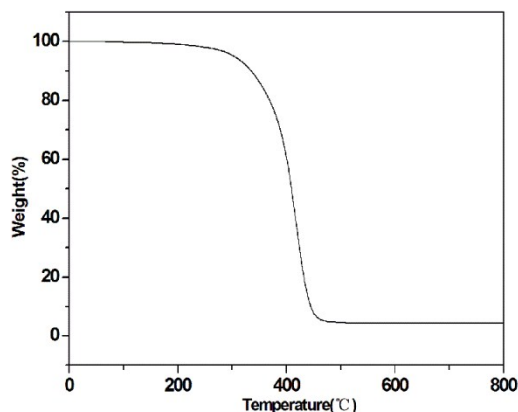
Fig. 9 TGA result of the photosensitive polyurethane with a heating rate of 10 ℃ min^{-1} in N$_2$ from 0 ℃ temperature to 800 ℃.

3.3 Properties of photosensitive polyurethane films

5 The charge transport process is believed to occur within the first few semiconducting layers in proximity to the gate dielectric[30]. Furthermore, the surface chemical group of gate dielectric, −OH, can affect the charge transport by deep trapping/doping or by scattering carriers at the semiconductor–dielectric interface. Note 10 that the photosensitive polyurethane films have relatively low water absorptions, as confirmed by the large aqueous contact angles (84.3°) (Figure 10). This result illustrates that a large number of reactive hydrogen in the structure of the obtained polymers did not exist in the film surface, thus implying that the 15 density of electron trapping is relatively low.

The surface morphologies of the dielectric layer are important to the performance of devices. The surface morphologies of the resulting polymer films were investigated by using atomic force microscope (AFM). The AFM images are shown in Figure 10. 20 The root-mean-square (RMS) roughness of the film was 0.334 nm, demonstrating that the photosensitive polyurethane could be very effective for producing extremely smooth surfaces. Furthermore, no crack or pin-holes were observed over different areas of the surface scanned by AFM.
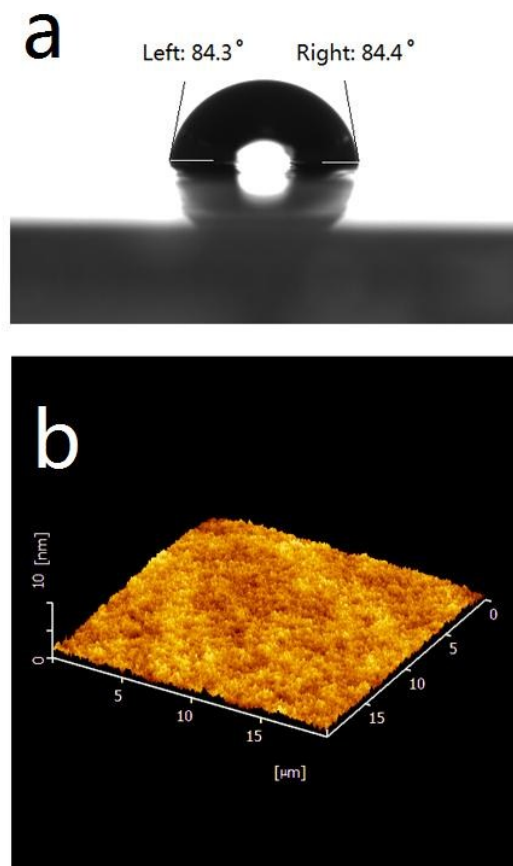

25 **Fig. 10** The tapping mode AFM image (10 × 10 μm^2 scan area) for evaluation of film surface morphology and the aqueous contact angle of the photosensitive polyurethane.

The photopatternability of the polyurethane was also investigated. 30 The polyurethane film was performed at the temperature of 80 ℃ for 10 min to remove the solvent, and then annealed at 120 ℃ for 3 min to improve the adhesion of the polyurethane and SiO$_2$ wafer. With 30 × 50 μm strip-type optical grating, the film was irradiated at room temperature by a high-pressure Hg lamp. After 35 UV-light exposure, the polyurethane was developed by dipping in a solution of 75% γ-butyrolactone and 25% xylene for 90 s at room temperature and followed by rinsing with ethanol to give a nice pattern. A field-emission scanning electron microscope image of a negatively patterned polyurethane thin film with a 40 resolution of 30 μm is shown in Figure 11. The bright area represents the developed part. These results indicate that the polyurethane has a excellent photosensitive property.
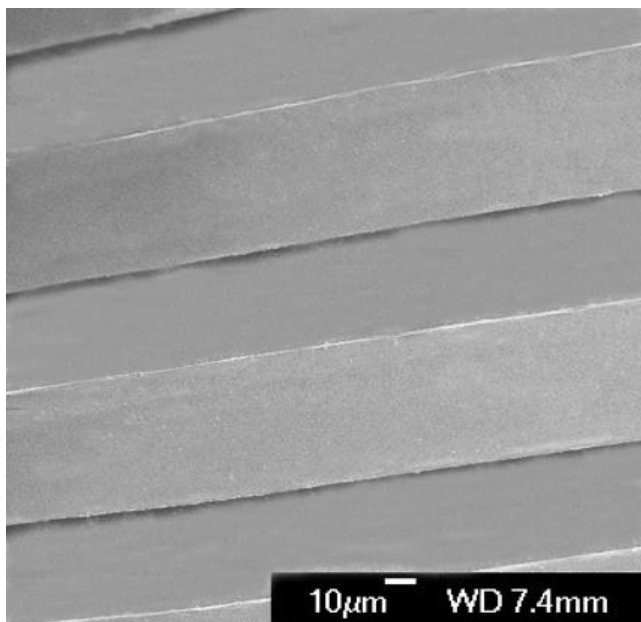
Fig. 11 SEM image of patterning polyurethane film.

3.4 Leakage current and capacitance of the photosensitive polyurethane film

5 The principal electrical characteristic of dielectric films was the

30 **Table 1** The parameters of the photosensitive polyurethane.

leakage current. The leakage current should be as low as possible in dielectric film and has a significant impact on the key transistor parameters, including on/off ratio and field-effect mobility. The dielectric characteristic of the photosensitive polyurethane film 10 were evaluated via the quantitative leakage current by an MIM capacitor. Figure 12 shows the leakage current density–electric voltage (*I–V*) plot, demonstrating that the cross-linked film exhibits the superior insulating properties than not cross-linked film. The leakage current was less than 1×10^{-5} A cm^{-2}. The lower 15 leakage current of the polymer films was achieved by the lower free volume and non-pinhole surface morphology.

The capacitance determines the number of charge carriers that can be induced in the semiconductor layer at a particular gate bias, as given by Formula 1:

$$C_i = \epsilon_0(k/d) \qquad (1)$$

where ϵ_0 is the vacuum permittivity, k is the dielectric constant, and d is the thickness of the dielectric layer. The formula indicates that the capacitance magnitude depends on k and d. The capacitance-frequency curve of the resulting photosensitive 25 polyurethane is plotted in Figure 13. From capacitance date, the capacitance (4.1 nF cm^{-2}) of the polyurethane film was obtained by the MIM structures, and dielectric constant of polyurethane was 3.2 at 100 kHz. The parameters of the photosensitive polyurethane and film are listed in Table 1.

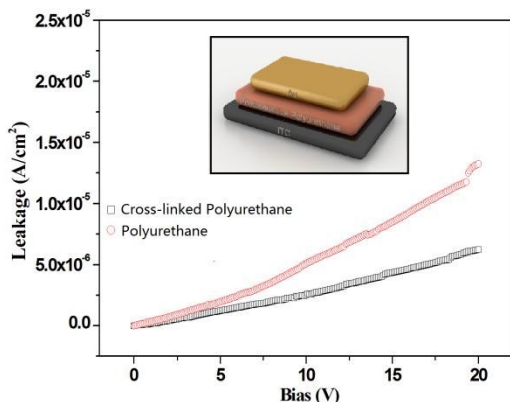|	molecular weight (Daltons)	Tg （℃）	RMS roughness (nm)	Aqueous contact angle (°)	Thickness (nm)	C$_i$ (nF/cm)	Dielectric constant (*k*)
Polyurethane	58290	123	0.334	84.3	690	4.1	3.2

Fig. 12 Leakage current density-bias voltage plot with polyurethane film as dielectric layer.
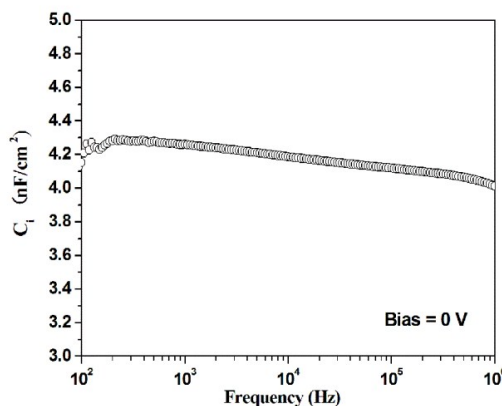

35 Fig. 13 Capacitance-frequency plot for the polyurethane film investigated in this study under 0 V bias voltages.

3.5 Properties of *p*-6P/VOPc organic thin-film transistors with photosensitive polyurethane films as dielectric layer

40 In a typical bottom-gate top-contact OTFT, the electron between the source and drain contact is modulated by both the source–gate voltage (V_{GS}) and the source-drain voltage (V_{SD}). When the device is in the on-state of the source–gate voltage relationship ($V_G > 0$ V), an abrupt increase in current must be achieved. In the off state 45 ($V_G = 0$ V), the channel current must be low. The saturation current in OTFTs is generally calculated as follows:

Journal Name

ARTICLE TYPE

$$I_{DS,sat} = \frac{C_i \mu W}{2L}(V_{GS} - V_{th})^2 \qquad (2)$$

where μ is the charge carrier mobility; V_{th} is the threshold voltage; W and L are the width and length of the OTFT channel, respectively.
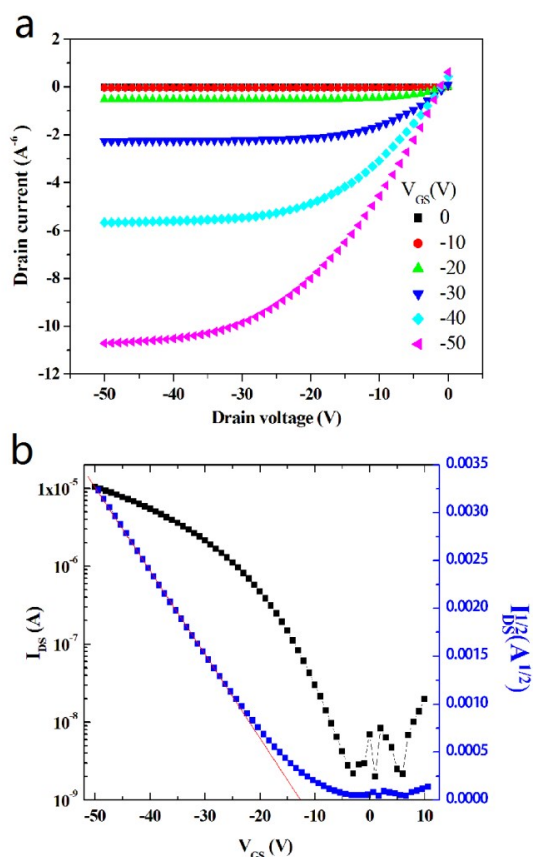

5

Fig. 14 Output characteristic curve and transfer characteristic curve of *p*-6P / VOPc OTFT with polyurethane film as dielectric layer.

The output characteristics (drain current vs. drain voltage, I_{DS} vs. V_{DS}) of the VOPc OTFTs are shown in Figure 14(a) for various

10 gate voltages. The OTFTs exhibit typical p-type characteristics with a transition from linear to saturation behavior in the device. At a given negative gate voltage (V_{GS}), I_{ds} initially increases linearly with a small negative V_{DS} and then saturates. Clear saturation behavior was observed for the OTFT device with the

15 cross-linked gate insulator. The transfer characteristics (drain current vs. gate voltage, I_{DS}-V_{GS}) are shown in Figure 14(b). When V_{GS} was swept from +10 to -50 V and V_{DS} was set at -50 V, the mobility of the VOPc OTFT with the photosensitive polyurethane as gate insulate was found to be 0.13 cm^2/Vs. The

20 data are summarized in Table 2.

Table 2 The electric parameters of the *p*-6P / VOPc OTFTs with novel Polyurethane as dielectric layer.

Insulating layer	μ (cm^2/Vs)	Vth (V)	On/Off
Polyurethane	0.13	-13	10^4

Conclusion

25 We have demonstrated that the novel photosensitive polyurethane is thermostable, smooth, pinhole free and insulating dielectric film. The film has been used to fabricate solution-processable OTFT devices. The results demonstrate that leakage current of polyurethane film can be minimized due to the reduced free

30 volume by the cross-link reaction of photosensitive groups. The novel solution-processable polyurethane dielectric film is a promising candidate for the exploration of OTFT devices.

ACKNOWLEDGMENT

Notes and references

1.Key Lab of Supramolecular Structure & Materials, College of Chemistry, Jilin University, Changchun 130012, PR China

40 *2.State Key Laboratory of Polymer Physics and Chemistry, Changchun Institute of Applied Chemistry, Chinese Academy of Sciences, Changchun 130012, PR China.*

† Electronic Supplementary Information (ESI) available: See DOI:10.1039/b000000x/

45 1   X. Zhao, S. Wang, A. Li, J. Ouyang, G. Xia, J. Zhou, *RSC Adv.*, 2014, **4**, 14890.
2   P. Lin, F. Yan, *Adv. Mater.*, 2012, **24**, 34.
3   D. Elkington, W. J. Belcher, P. C. Dastoor, X. J. Zhou, *Appl. Phys. Lett.*, 2014, **105**, 043303.
50 4   Y. Li, H. Wang, Z. Shi, J. Mei, X. Wang, D. Yan, Z. Cui, *Polym. Chem.*, 2015, **6**, 6651.
5   A. Facchetti, M. Yoon, T. J. Marks, *Adv. Mater.*, 2005, **17**, 1705.
6   W. Y. Chou, T. Y. Ho, H. L. Cheng, F. C. Tang, J. H. Chen, Y. W. Wang, *RSC Adv.*, 2013, **3**, 20267.
55 7   J. Yang, H. Wang, T. Wang, F. Zhu, G. Li, D. Yan, *J. Phys. Chem. B*, 2008, **112**, 7816.
8   H. Wang, F. Zhu, J. Yang, Y. Geng, D. Yan, *Adv. Mater.*, 2007, **19**, 2168
9   H. Wang, D. Song, J. Yang, B. Yu, Y. Geng, D. Yan, *Appl. Phys.*
60 *Lett.*, 2007, **90**, 253510.
10 C. Nanjo, T. Fujimoto, M. M. Matsushita, K. Awaga, *J. Phys. Chem. C*, 2014, **118**, 14142.
11 Y. Hou; Y. Deng, Y. Wang, H. Gao, *RSC Adv.*, 2015, **5**, 72090.
12 T. H. Huang, K. C. Liu, Z. Pei, W. K. Lin, S. T. Chang, *Org.*
65 *Electron.*, 2011, **12**, 1527.
13 Y. G. Ha, M. G. Kim, A. Facchetti, T. J. Marks, *J. Am. Chem. Soc.*, 2010, **132**, 17426.
14 J. H. Bae, Y. Choi, *Solid-State Electron.*, 2012, **72**, 44.
15 I. Yutaka, A. A. Virkar, S. Mannsfeld, J. H. Oh, M. F. Toney, Z. Bao,
70 *J. Am. Chem. Soc.*, 2009, **131**, 9396-9404.

RSC Advances Accepted Manuscript

16 Y. G. Ha, J. D. Emery, M. J. Bedzyk, H. Usta, A. Facchetti, T. J. Marks, *J. Am. Chem. Soc.*, 2011, **133**, 10239.

17 S. R. Walter, J. Youn, J. D. Emery, S. Kewalramani, J. W. Hennek, M. J. Bedzyk, A. Facchetti, T. J. Marks, F. M. Geiger, *J. Am. Chem. Soc.*, 2012, **134**, 11726.

18 K. C. Liao, A. G. Ismail, L. Kreplak, J. Schwartz, I. G. Hill, *Adv. Mater.*, 2010, **22**, 3081.

19 J. A. Cheng, C. S. Chuang, M. N. Chang, Y. C. Tsai, H. P. D. Shieh, *Org. Electron.*, 2008, **9**, 1069.

20 G. Nunes, S. G. Zane, J. S. Meth, *J. Appl. Phys.*, 2005, **98**, 104503.

21 X. Sun, L. Zhang, C. A. Di, Y. Wen, Y. Guo, Y. Zhao, G. Yu, Y. Liu, *Adv. Mater.*, 2011, **23**, 3128.

22 J. Li, Z. Sun, F. Yan, *Adv. Mater.*, 2012, **24**, 88.

23 M. E. Roberts, N. R. Queraltó, S. C. B. Mannsfeld, Z. Bao, *Chem. Mater.*, 2009, **21**, 2292

24 H. Kim, J. H. Bae, S. D. Lee, G. Horowitz, *Org. Electron.*, 2012, **13**, 1255.

25 M. Li, Z. Jin, N. Cernetic, J. Luo, Z. Cui, A. K. Y. Jen, *Polym. Chem.*, 2013, **4**, 4434.

26 Y. Li, H. Wang, C. Zhang, Y. Zhang, Z. Cui, D. Yan, Z. Shi, *Polym. Chem.*, 2015, **6**, 3685.

27 D. Fan, X. Fei, J. Tian, L. Xu, X. Wang, S. Fan, Y. Wang, *Polym. Chem.*, 2015, **6**, 5430.

28 C. Y. Zhang, Z. C. Cui, H. Wang, D. H. Yan, Y. Li, Z. S. Shi, A. Wu, Z. Zhao, S. Luan, *Org. Electron.*, 2014, **15**, 2295.

29 C. Y. Zhang, H. Wang, Z. S. Shi, Z. C. Cui, D. H. Yan, *Org. Electron.*, 2012, **13**, 3302.

30 C. K. Myung-Han Yoon, A. Facchetti, Tobin J. Marks, *J. Am. Chem. Soc.*, 2006, **128**, 12851.

The solution-processable photosensitive polyurethane dielectric film is a promising candidate for the exploration of organic thin-film transistors (OTFTs).

Novel Photosensitive Polyurethane

A bottom-gate top-contact para-sexiphenyl (*p*-6P) / vanadyl-phthalocyanine (VOPc) OTFTs